The SGLT-2 inhibitor empagliflozin improves myocardial strain, reduces cardiac fibrosis and pro-inflammatory cytokines in non-diabetic mice treated with doxorubicin

Vincenzo Quagliariello (quagliariello.enzo@gmail.com)
Istituto Nazionale Tumori IRCCS Fondazione Pascale https://orcid.org/0000-0002-4557-5401
Michelino De Laurentiis
Istituto Nazionale Tumori IRCCS Fondazione Pascale
Domenica Rea
Istituto Nazionale Tumori IRCCS Fondazione Pascale
Antonio Barbieri
Istituto Nazionale Tumori IRCCS Fondazione Pascale
Maria Gaia Monti
University of Naples Federico II: Universita degli Studi di Napoli Federico II
andreina carbone
Istituto Nazionale Tumori IRCCS Fondazione Pascale
Andrea Paccone
Istituto Nazionale Tumori IRCCS Fondazione Pascale
Maria Laura Canale
Versilia Hospital: Ospedale Versilia
Gerardo Botti
Istituto Nazionale Tumori IRCCS Fondazione Pascale
Nicola Maurea
Istituto Nazionale Tumori IRCCS Fondazione Pascale

Research Article

Keywords: Empagliflozin, Cardio-Oncology, Doxorubicin, Inflammation, Interleukins

Posted Date: February 25th, 2021

DOI: https://doi.org/10.21203/rs.3.rs-245054/v1

Version of Record: A version of this preprint was published at Cardiovascular Diabetology on July 23rd, 2021. See the published version at https://doi.org/10.1186/s12933-021-01346-y.

Abstract

Background

Empagliflozin, a selective inhibitor of the sodium glucose co-transporter 2, reduced the risk of hospitalization for heart failure and cardiovascular death in type 2 diabetic patients in the EMPA-REG OUTCOME trial. Recent trials evidenced several cardio-renal benefits of empagliflozin in non-diabetic patients through the involvement of biochemical pathways that are still to be deeply analyzed . We aimed to evaluate the effects of empagliflozin on myocardial strain of non-diabetic mice treated with doxorubicin (DOXO) through the analysis of NLRP3 inflammasome and Myd88-related pathways resulting in anti-apoptotic and anti-fibrotic effects.

Methods

Preliminary cellular studies were performed on mouse cardiomyocytes (HL-1 cell line) exposed to doxorubicin alone or combined to empagliflozin. The following analysis were performed: determination of cell viability (through a modified MTT assay), study of intracellular ROS production, lipid peroxidation (quantifying intracellular malondialdehyde and 4-hydroxynonenal), intracellular Ca^{2+} homeostasis. Moreover, pro-inflammatory studied were also performed: expression of NLRP3 inflammasome, MyD88 myddosome and p65/NF-κB associated to secretion of cytokines involved in cardiotoxicity (Interleukins 1β, 8, 6). C57Bl/6 mice were untreated (Sham, n=6) or treated for 10 days with doxorubicin (DOXO, n=6), empagliflozin (EMPA, n=6) or doxorubicin combined to empagliflozin (DOXO-EMPA, n=6). DOXO was injected intraperitoneally. Radial and longitudinal strain were analysed through transthoracic echocardiography (Vevo 2100). Cardiac fibrosis and apoptosis were histologically studied through Picrosirius red and TdT-mediated dUTP nick-end labelling (TUNEL) assay, respectively. Tissue NLRP3, Myd88 and cytokines were quantified after treatments.

Results

Cardiomyocytes exposed to doxorubicin increased the intracellular Ca^{2+} content and expression of several pro-inflammatory markers associated to cell death; co-incubation with empagliflozin reduced significantly the magnitude of the effects. In preclinical study, empagliflozin prevented the reduction of radial and longitudinal strain after 10 days of treatment with doxorubicin (radial strain (RS) 30.3 % in EMPA-DOXO vs 15.7% in DOXO mice ; longitudinal strain (LS) -17% in EMPA-DOXO vs -11,7% in DOXO mice ($p<0.001$ for both). A significant reduction of cardiac fibrosis and apoptosis were also seen. A reduced expression of pro-inflammatory cytokines, NLRP3, MyD88 and NF-kB in heart, liver and kidneys was also seen in DOXO-EMPA group compared to DOXO mice ($p<0.001$)

Conclusion

Empagliflozin reduced fibrosis, apoptosis and inflammation in doxorubicin-treated mice through the involvement of NLRP3 and MyD88-related pathways, resulting in a significant improvement of

myocardial strain. These findings provides the proof of concept for translational studies designed to reduce adverse cardiovascular outcomes in non-diabetic cancer patients treated with doxorubicin.

Background

Doxorubicin (DOXO) induced-cardiotoxicity is a well known adverse event in cancer patients [1-2]. As recently described in literature, DOXO-induced cardiotoxicity involves pro-inflammatory interleukins, pro-oxidative markers, ferroptosis, topoisomerase IIβ inhibition and mitochondrial dysfunction [3,4,5]. Improvement in knowledge of DOXO-induced pathophysiology pushes the search for new potential cardioprotective agents able to prevent cardiotoxic events.

Empagliflozin (EMPA) (Jardiance, Boehringer Ingelheim) is a sodium-glucose cotransporter 2 (SGLT-2) inhibitor with hypoglycaemic and anti-oxidant effects [6]. The beneficial properties of empagliflozin involves both indirect and direct effects in heart tissue, such as the reduction of 8-iso prostaglandin f2α (a product of lipid peroxidation), blunted the activation of mitogenic stress pathways such ERKs, JNKs, and p38 MAPKs [7].

In EMPA-REG Outcome trial, which enrolled about 7000 patients affected by type 2 diabetes, deaths from cardiovascular causes was 3.7 % in patients treated with empagliflozin versus 5.9 % in patients receiving placebo, which corresponds to a relative risk reduction of cardiovascular diseases of 38% [8-9-10]. Interestingly, empagliflozin exerts beneficial effects also in non-diabetic patients, as described in recent clinical trials named EMPEROR-Reduced/preserved [11] .

Given the crucial role of the heart pro-inflammatory microenvironment in the genesis of DOXO-related cardiotoxicity, we evaluated the impact of empagliflozin on DOXO-induced cardiotoxicity and studied the putative beneficial effects on fibrosis, longitudinal and radial strain and expression of pro-inflammatory cytokines both in cardiomyocytes and mouse models.

Methods

Cell viability

Firstly, we aimed to evaluate the effects of empagliflozin combined to DOXO in cell cultures of cardiomyocytes (HL-1 adult mouse cells derived from American Type Culture Collection, Manassas, VA, USA), estrogen-responsive and triple-negative breast cancer cells (MCF-7 and MDA-MB-231 cell lines, derived from American Type Culture Collection, Manassas, VA, USA). To evaluate the cytotoxic or cytoprotective effects of empagliflozin, the mitochondrial dehydrogenase activity was quantified through a modified MTT [3-(4,5-dimethyldiazol-2-yl)-2,5- diphenyltetrazoliumbromide] method, called MTS assay, according to the manufacturer's instructions (Dojindo Molecular Technologies Inc., Rockville, MD, USA) [12]. Briefly, HL-1 cells were grown in a complete medium constituted by Claycomb medium, 10% V/v heat-inactivated foetal bovine serum, 2 mM l-glutamine, 100 U/ml penicillin and 100 µg/ml streptomycin in 96-well plates (density of 10,000 cells/well) at 37°C in a humidified 5% CO_2 atmosphere. MCF-7 human

breast cancer cells (ERα+, PR+, HER2-) were cultured in Dulbecco's modified Eagle's medium (DMEM) supplemented with 10% fetal bovine serum (FBS), 2 mM glutamine, 100 units/mL penicillin and 100 units/mL streptomycin. Triple negative MDA-MB-231 (ATCC® HTB-26™) cells were grown in ATCC-formulated Leibovitz's L-15 Medium supplemented with 10% fetal bovine serum (FBS) (HyClone™, GE Healthcare Life Sciences, Milan, Italy) and Penic illin-Streptomycin (100 U/mL, Gibco®, Milan, Italy). Cell cultures were maintained in a humidified atmosphere of 95% air and 5% CO2 at 37 °C.

After 24 hours of appropriate growth, cells were exposed to: DOXO (0.1 to 50 μM); EMPA (50, 100 and 500 nM); DOXO-EMPA (both drugs combined). Cells were than incubated for 24 hours with each drug under standard growth conditions. Cells were then washed three times with phosphate buffered solution (PBS) at pH 7.4 and then incubated with 100 μl of an MTT solution (0.5 mg/ml in cell culture medium) for 4 hours at 37°C. Absorbance readings were acquired at a wavelength of 450 nm with the Tecan Infinite M200 plate-reader (Tecan Life Sciences Home, Männedorf, Switzerland) using I-control software (Tecan). Relative cell viability (%) was calculated with the following formula [A]test/[A]control×100, where "[A]test" is the absorbance of the test sample, and "[A]control" is the absorbance of the control cells incubated solely in culture medium.

Quantification of intracellular reactive oxygen species (iROS)

Quantification of iROS was performed by using a conventional fluorescent probe (DCFH-DA) as described elsewhere [13]. Cardiomyocytes ($5x10^3$ cells/well) were seeded in a 24-well plate and allowed to grow for 24 hours; after, cells were pre-treated or not with EMPA at 10, 50 and 500 nM for 4 hours. Cardiomyocytes pre-treated with gallic acid (50 μM) served as positive control. After, cells were incubated with 5 μM DCFH-DA in PBS for 30 minutes. Then, DCFH-DA was removed from each well and cells were stimulated with 40 ng/mL of lipopolysaccharides (LPS, as internal control) or DOXO at 100 nM for 12 hours. Cell fluorescence was measured using a microplate spectrofluorometer. Intracellular antioxidant activity was expressed as percentage of control cells. The concentration of DOXO used were within the range of 25–250 nM, calculated for steady-state plasma concentrations of DOXO, intravenously administered, in cancer patients at the common therapeutic dosage of 15–90 mg/m^2 [14,15].

Lipid peroxidation

To study the putative anti-oxidant effects of empagliflozin, HL-1 cells were grown as described above. Subsequently, $5x10^3$ cells/well were seeded in a 24-well plate and allowed to grow for 24 hours and exposed to DOXO (100 nM) or LPS (40 ng/ml, as positive control in inflammation in human cells, as described by our group [12,13]) for 6 hours or pre-treated for 4 hours with EMPA (10, 50 and 500 nM) or with gallic acid (50 μM) as anti-oxidant positive control. After centrifugation at 800× g for 5 minutes, the supernatant was evaluated for malondialdehyde (MDA) and 4-hydroxy 2-hexenal (4-HNA) using commercial kits with a spectrophotometer according to the manufacturer's protocols (Sigma Aldrich, Milan, Italy).

Nitric oxide assay

To evaluate the effects of empagliflozin on the release of nitric oxide from HL-1 cells, we analysed the release of nitrite, which is a stable product of nitric oxide in aqueous medium, using the Griess Reagent System (Promega, Madison, WI, USA) as described elsewhere [16]. Cells were treated as described before; after treatment, the culture medium was then mixed with an equal volume of sulfanylamide solution (1% v/v in 5% v/v phosphoric acid) and of N-1-naphtylethylenediamine dihydrochloride solution (0.1% v/v in water). Absorbance was measured at 540 nm with a spectrophotometer

Intracellular Ca^{2+} assay

Cardiomyocytes exposed to DOXO increases the intracellular calcium concentration due overproduction of iROS [17]. We quantified the intracellular Ca^{2+} in HL-1 cells by using the fluorescence dye Fluo-3 AM, according to the manufacturer's protocol. Cardiomyocytes were untreated or treated as described before. After incubation, cells were loaded with 5 μM Fluo-3 AM at 37˚C for 30 minutes in the dark, and then washed three times with PBS (pH 7.4) to remove the excess dye. Fluo-3 chelated with calcium produces fluorescence that was quantified with a spectrofluorometer at excitation and emission wavelengths of 488 nm and 525 nm, respectively.

Anti-inflammatory studies

Cytokine assay

The expression of IL-6, IL-8 and IL-1β was performed through ELISA method, as described elsewhere [12]. Briefly, HL-1 cells were grown as described above. After incubation for 24 hours and starvation in serum-free medium for 2.5 hours, HL-1 cells were treated or not with EMPA in doses ranging from 10 to 500 nM for 4 hours before exposure to LPS (40 ng/ml) or DOXO (100 nM) for 12 hours to stimulate inflammation. After exposure, supernatants were collected, centrifuged to pellet any detached cells and measured using IL-1β, IL-6 and IL-8 ELISA kits according to the manufacturer’s instructions (Sigma Aldrich, Milan, Italy).

Leukotriene B4 assay

To quantify leukotrienes B4 (LTB4), cardiomyocytes were treated as described before; after treatments, cells were incubated at 37°C for 30 minutes with serum-free medium containing a solution constituted by 5 μM of the calcium ionophore A23187, 1.6 mM of CaCl2 and 10 μM of arachidonic acid. Arachidonate was used as precursor of leukotriene synthesis. Immuno reactive LTB4 was quantified with an ELISA procedure (Cayman Chemical) according to the supplier's instructions [18].

p65/NF-kB expression

Cardiomyocytes were treated with DOXO (100 nM) or EMPA (10, 50 and 500 nM) or DOXO and EMPA for 24 hours. After, nuclear extracts were analysed using the TransAM p65/NF-κB transcription factor assay kit (Active Motif, Carlsbad, CA, USA), according to the manufacturer’s recommendations [19]. Data were expressed as the percentage of p65/NF-kB DNA binding versus control (untreated) cells.

NLRP3 and MyD88 expression

Cardiomyocytes were treated with DOXO (100 nM) or EMPA (10, 50 and 500 nM) or DOXO and EMPA for 24 hours. After treatments, cells were harvested and lysed in complete lyses buffer (50 mM Tris-HCl, pH 7.4, 1 mM EDTA, 100 mM NaCl, 20 mM NaF, 3mM Na3 VO4, 1mM PMSF, and protease inhibitor cocktail). After centrifugation, supernatants were collected and treated to the quantification of MyD88 (Mouse MyD88 ELISA Kit, Abcam, Italy) and NLRP3 (Mouse NLRP3 ELISA Kit, Aviva Systems Biology). For mouse MyD88 ELISA the sensitivity was < 10 pg/ml and range of detection was 156pg/ml - 10000 pg/ml; for mouse NLRP3 ELISA assay, the sensitivity was < 0.078 ng/mL and range of detection was 0.156 – 10 ng/mL.

Confocal laser scanning microscope (CLSM) imaging

HL-1 cells were cultured as described above. After, $5x10^3$ cells/well were seeded in a 24-well plate and allowed to grow for 24 hours and untreated (control) or treated with DOXO (100 nM) or EMPA (100 nM) or DOXO (100 nM) combined with EMPA (100 nM) for one day. Then, cells were thoroughly rinsed three times with PBS and fixed with 2.5% glutaraldehyde in PBS for 20 minutes, as described elsewhere [20]. After washing three times with PBS, cells were permeabilized with 0.1% Triton-X100 in PBS for 10 minutes and then washed three times with PBS. Subsequently, cells were blocked with 1% BSA in PBS for 20 minutes. After three washes with PBS, cells were incubated with a Rabbit polyclonal antibody against p65/NF-kB (clone ab16502 Abcam) diluted 1:200 in 1% BSA for 1 hour. After washing, cells were incubated for 1 hour with Goat Anti-Rabbit secondary antibody IgG H&L (FITC) (clone ab6717, AbCam) diluted 1:1000 in 1% BSA. Nuclear staining was obtained through the use of NUCLEAR-ID® Red DNA stain (Enzo Life Technology, Milan, Italy) diluted 1:2000 in PBS for 15-30 minutes at 37°C. After washing in PBS, cells were blocked with 1% BSA in PBS for 20 minutes. A confocal microscope (C1 Nikon) equipped with EZ-C1 software for data acquisition was used (60x oil immersion objective). Expression of p65/NF-kB and nucleus were imaged through excitation/emission at 492/518 nm and 566/650 nm, respectively.

Animal models

Twenty-four female C57Bl/6 mice were purchased from Harlan, San Pietro al Natisone (Italy). Mice were housed 6 per cage and maintained on a 12 hour light-12 hour dark cycle (lights on at 7.00 am) in a temperature-controlled room (22±2°C) and with food and water ad libitum. Preclinical experimental protocols were in accordance with EU Directive 2010/63/EU for animal experiments, and Italian D.L.vo 26/2014 low; were approved by Ministry of Health with authorization number 1467/17-PR of the 13-02-2017, and institutional ethics committees: Organismo preposto al benessere degli animali (OPBA). After 1 week of growth, mice were randomized for weight-adjusted treatment. Mice were divided in 4 experimental groups (n=6/group) (i) 100 µl saline solution (Sham); (ii) DOXO at 2.17 mg/kg/day through intraperitoneal administration (i.p) ; (iii) EMPA 10 mg/kg/day through oral gavage; (iv) EMPA/DOXO in combination (at the same concentration of each drug tested alone).Treatments were performed according to our protocol recently published were we evaluated the cardioprotective effects of Ranolazine against cardiotoxicity of doxorubicin for 10 days [21] ; in fact, also in this case, in group of combinatorial

treatment EMPA/DOXO, mice were treated with empagliflozin alone for 3 days and the remaining 7 days also in combination to DOXO. Another work investigated on the initial damages of doxorubicin and trastuzumab administration at low doses in mice with significant changes in cardiac apoptosis, necrosis and fibrosis leading to reduced cardiac functions after 7 days of treatment [22]. Notably, used short-term treatment of doxorubicin is more than sufficient to evaluate myocardial dysfunction in mice; in fact, in the same experimental procedure showed by Tocchetti G et al. [21], and Fedele et al., [23] in C57BL6 mice, doxorubicin treatment for 7 days produced left ventricular dilation and decreased echo-measured fractional shortening (FS) as well as detectable apoptosis and inflammation in myocardial tissues.

Transthoracic echocardiography

To assess cardiac function in vivo we performed non-invasive transthoracic echocardiography in sedated mice using a Vevo 2100 high-resolution imaging system (40-MHz transducer; Visualsonics, Toronto, ON, Canada) as described in literature [22,24]. Mice were anaesthetized with tiletamine (0.09 mg/g), zolazepam (0.09 mg/g), and 0.01% atropine (0.04 mL/g). After, animals were sedated and placed in supine position on a temperature-controller surgical table to maintain rectal temperature at 37°C, continual ECG monitoring was obtained via limb electrodes. Cardiac function was evaluated at basal conditions and at 2 and 10 days of treatments. Left ventricular echocardiography was assessed in parasternal long-axis views at a frame rate of 233 Hz. Notably, we measured the strain in parasternal views because the apical view is difficult to perform in small animal [25] ; this method was in line with other studies for STE analyses that were performed on parasternal long-axis B-mode loops using a VisualSonics Vevo 2100 system (VisualSonics) [26,27,28]. Image depth, width, and gain settings were optimized to improve image quality. End-systole and end-diastole dimensions were defined as the phases corresponding to the ECG T wave, and to the R wave, respectively. M-mode LV internal dimensions, diastolic (LVID,d) and LV internal dimensions, systolic (LVID,s) were averaged from 3 to 5 beats. LVID,d and LVID,s were measured from the LV M-mode at the mid papillary muscle level. Fractional shortening percentage (% FS) was calculated as [(LVID, d-LVID, s)/LVID, d] X 100, and ejection fraction percentage (% EF) was calculated as [(EDvol-ESvol)/EDvol] X100. The strain was expressed as percentage. The analysis start with acquired B-mode loops and were imported into the Vevo Strain software. Three consecutive cardiac cycles were selected and the endocardium traced. Upon adequate tracing of the endocardium, an epicardial trace was added. ST based strain allowed assessment of strains specific to 6 myocardial segments per LV view. Internally, 10 or plus points were measured for each of the 6 segments, resulting in 48 data points in total. Strain and SR are useful in the detection of regional myocardial function. The strain is evaluated on long-axis views as well as: radial and longitudinal. Radial strain (RS), defined as the percent change in myocardial wall thickness is a positive curve reflecting increasing myocardial thickness during systole and diminishing wall thickness during diastole and represent myocardial deformation toward the center of the LV cavity. Longitudinal strain (LS) detects the percent change in length of the ventricle, typically measured from the endocardial wall in the long-axis view. Myocardial deformation rate, expressed in 1/s, was also calculated. Notably, we measure LV , diastolic and systolic volumes in the one-dimensional view following the proper instructions of " Small Animal Echocardiography using the Vevo® 2100 Imaging System" [29] and also in agree with our previous similar work [21].

Anti-inflammatory studies in tissue extracts

After treatments, heart, liver and left kidney were weighed and treated for quantification of cytokines, MyD88 and NLRP3. The heart tissues were cut in transverse section into two parts. The basal parts of the hearts, and the whole liver and left kidney were snap-frozen in dry ice until tissue homogenization, which was carried out in 0.1 M PBS (pH 7.4) containing 1% Triton X-100, protease inhibitor cocktail and processed using a high intensity ultrasonic liquid processor. The homogenates were centrifuged at 4^{o}C and supernatants were used to determine tissue markers. The apical parts of the heart sections were fixed in 10% neutral buffered formalin for 48 h for the cardiac fibrosis and apoptosis assays Methods for quantification in interleukins in tissue extracts were followed using the appropriate ELISA kits for mouse IL-1β, IL-8 and IL-6 detections, as used in the cellular experiments, according to the manufacturer's instructions; results are expressed as pg of interleukin/mg of tissue. The MyD88 and NLRP3 expression in heart tissues were performed through the use of the same kits described for cellular experiments and results are expressed as pg of MyD88 or pg of NLRP3/mg of protein.

Cardiac fibrosis and collagen

For ex vivo analyses, hearts were excised and fixed in 10% neutral buffered solution. The myocardial tissue was formalin-fixed and paraffin-embedded for morphometry and immunohistochemistry. General morphology was studied using haematoxylin-eosin staining. To measure collagen content, we deparaffinised 6 µm-thick cross sections and stained them with Picrosirius red (Carlo Erba Laboratories, Milan, Italy). The collagen volume fraction was expressed as the mean percentage of Picrosirius red-stained tissue areas divided by total tissue area in the same field, and was evaluated in 15 fields at 60× magnification. The positively stained (red) fibrotic area was measured with a computer-assisted image analysis system (Nikon NIS Elements. Nikon Instruments, Melville, NY, USA). To measure capillary density, we incubated sections overnight with biotinylated Bandeira easimplicifolia Isolectin-I (Sigma-Aldrich Co., St Louis, MO, USA) followed by tyramide signal amplification enhancement (PerkinElmer Inc., Waltham, MA, USA). Capillaries were visualized by 3,3'-diaminobenzidine tetrahydrochloride, counted and expressed as the number of capillaries per mm^{2}.

Cardiac apoptosis

Cardiac sections measuring 6 µm were examined for the presence of apoptotic cardiomyocytes by TdT-mediated dUTP nick-end labelling (TUNEL) assay using a Promega Dead End™ colorimetric TUNEL system (Promega, Madison, WI, USA) with a streptavidin-peroxidase system. Controls were obtained by omitting the TdT enzyme from the reaction mixture. The percentage of TUNEL-positive myocytes was determined by counting 10 random fields per section under a microscope (Nikon NIS Elements). Using this procedure, apoptotic nuclei were stained dark brown. Labelled nuclei were counted and expressed as the percentage of positively stained cells.

SGLT-2 expression through western blot analysis

Same studies indicated that human and murine cardiomyocytes express SGLT-2 [30]. To confirm this data, we analysed SGLT-2 expression in cardiomyocytes and heart tissue of mice. Proteins were extracted using a lysis buffer containing protease- and phosphatase-inhibitors. Cell lysates were separated by SDS-PAGE and transferred onto nitrocellulose membrane. After treatment with 5% non-fat milk, these were first incubated overnight at 4 °C with primary antibody against SGLT2 then with secondary antibody and finally measured by enhanced chemiluminescence. GAPDH was used as internal control.

Statistical analyses

Continuous data were expressed as mean ± SD. Nonparametric tests were used both for paired and unpaired comparisons. Repeated measures ANOVA was used for all baseline to end-of-study comparisons. A p value < 0.05 was considered significant.

Results

Cell viability and calcium homeostasis

Incubation with DOXO decreased the viability of cardiomyocytes in a concentration-dependent manner, with an IC_{50} below 10 μM, whereas DOXO and EMPA co-incubation increased cell viability (Figure 1, A) . For example, the viability of cardiomyocytes exposed to DOXO at 50 μM plus EMPA at 10, 50 or 500 nM was 21.8%, 53.1% and 71%, respectively, higher than that of cardiomyocytes exposed to DOXO alone. In addition, cell viability was 18.8% higher in cardiomyocytes treated with EMPA alone at 500 nM than in control cells (*Figure 1B*). Moreover, $[Ca^{2+}]i$ (intracellular calcium) production was significantly higher in cardiomyocytes treated with DOXO and lipopolysaccharides (LPS) than in untreated cells ($p<0.001$ for both) (*Figure 1C*). At 24 hours of incubation, the mean $[Ca^{2+}]i$ of cardiomyocytes incubated with DOXO and EMPA at 10, 50 and 500 nM, was about 8%, 40% and 53% lower than the mean $[Ca^{2+}]i$ in cells treated with DOXO alone ($P<0.001$) (*Figure 1C*). The same results were obtained under pro-inflammatory conditions in LPS- and LPS/EMPA-treated cells (*Figure 1C*). As control, we evaluated the effects of EMPA on the anticancer efficacy of DOXO in human estrogen-responsive (*Figure 1, D*) and triple negative breast cancer cells (*Figure 1, E*); in line with literature [31], EMPA did not affects the anticancer effects of DOXO in breast cancer cells, indeed, at some concentrations it seems to increase slightly the cytotoxicity of DOXO. These preliminary results, although already confirmed by recent research [31], are of great interest and will be the performed by our group in further in-depth studies.

Intracellular reactive oxygen species (iROS), nitric oxide and lipid peroxidation

Exposure to LPS or DOXO alone increased the iROS content of 2.1 - and 2.6-fold, respectively, compared to untreated cells (*Figure 2 A*). Levels of iROS were 12%, 33.8% and 62.5% lower in cells treated with EMPA / DOXO than DOXO alone ($P<0.001$ for all). Notably, the anti-oxidant effects of EMPA at 50 nM were comparable to those of gallic acid, which is a common bioactive anti-oxidant compound (*Figure 2A*). EMPA significantly decreased the production of the lipid peroxidation markers MDA and 4-HNA in cardiomyocytes under pro-inflammatory conditions (*Figure 2B*). Lipid peroxidation was two-fold higher in

cardiomyocytes treated with DOXO than in untreated cardiomyocytes (p<0.001). DOXO and EMPA at 10, 50 and 500 nM decreased the production of MDA and 4-HNA by 14% and 11% (p<0.001 for both), 24% and 26% (p<0.001 for both), 49% and 35% (p<0.001 for both), respectively, compared to cells treated with DOXO alone (*Figure 2B*). Combination treatment of EMPA/DOXO reduced significantly the nitric oxide production (involved in pathogenesis of cardiovascular diseases [32,33]) compared to cells exposed to DOXO (*Figure 2C*).

Quantification of cytokines

Interleukin-8 was 2.5-fold higher in cardiomyocytes exposed to DOXO than in untreated cells (*Figure 3A*). Treatment with EMPA at 10, 50 and 500 nM resulted in a decrease of interleukin 8 of 8.8% (p<0.05), 24% (p<0.001) and 43% (p<0.001) versus DOXO alone. Interleukin-6, one of the most studied cytokine involved in cardiovascular diseases and cancer progression [34,35,36], decreased significantly in cells exposed to EMPA/DOXO (12.4%, 21% and 49.5%, at 10, 50 and 500 nM, respectively, p<0.001 for all), compared to cardiomyocytes exposed to DOXO alone (*Figure 3B*). Moreover, as shown in *Figure 6C*, EMPA at 10, 50 and 500 nM reduced the production of interleukin 1-β by 13%, 26% and 48%, respectively (p<0.001) compared to cells treated with DOXO alone (*Figure 3C*).

Leukotriene B4 assay

Leukotrienes B4 production was 3.4 times higher in cells treated with arachidonic acid than in untreated cells (125.3 ± 5.7 pg/ml vs 36.4 ± 6.7 pg/ml; p<0.001) (Figure 3, D). Pre-treatment with EMPA at 10, 50 and 500 nM reduced the production of leukotrienes by 7% (not significant), 16% (p<0.05) and 33% (p<0.001) versus cells exposed to arachidonic acid alone (*Figure 3D*). Leukotrienes B4 production was 4.3 times higher in cells treated with DOXO than in untreated cells (p<0.001). Notably, leukotriene B4 production was 24%, 33% and 50% lower in cardiomyocytes treated with DOXO and EMPA at 10, 50 and 500 nM, respectively than in cells exposed to DOXO alone.

p65/NF-kB assay

EMPA decreased the NF-κB activation in a dose-dependent manner in cardiomyocytes compared to untreated cells (*Figure 3 E*). Treatment with EMPA at 10, 50 and 500 nM decreased NF-κB activation by 16% (p<0.05), 32% (p<0.05) and 53% (p<0.001) versus cells exposed to DOXO. The same effects of empagliflozin were recently described by Andreadou I et al., [37].

MyD88 and NLRP3 expression

The MyD88 complex, also called myddosome and NLRP3 are analysed in cardiac cells exposed to DOXO and EMPA; as shown in *Figure 3F*, DOXO strongly increased both pro-inflammatory markers (p<0.01 for both), in agree with other preclinical studies. Treatment with EMPA decreases significantly Myd88 and NLRP3 indicating their involvement in cardiovascular beneficial effects of SGLT2 inhibitor during DOXO therapy.

Confocal scanning laser microscope imaging

Cellular imaging confirms the anti-inflammatory effects of EMPA. Cardiomyocytes exposed to DOXO increased significantly the p65/NF-kB expression (*Figure 3 G*) and nuclear localization compared to untreated cells (*Figure 3 A*); notably, exposed to EMPA decreased significantly the staining of p65/NF-kB in both in nuclear and cytosol of the cells, indicating anti-inflammatory effects.

Preclinical studies

Effects on pro-inflammatory cytokines, radial and longitudinal strain, cardiac fibrosis and apoptosis

As expected, IL-8, 6 and 1-β expression was significantly higher in the heart, liver and kidney of mice treated with DOXO compared to untreated mice ($p<0.005$ for all) (*Figure 4*). Cytokines were significantly lower in EMPA-treated mice than in DOXO-treated mice ($p<0.001$ for all). Specifically, IL-1β, IL-6 and IL-8 cardiac expression were 51%, 52% and 54.2% lower, respectively, in EMPA-treated mice than in DOXO-treated mice. In liver, the expression of IL-1β, IL-6 and IL-8 was 45%, 56% and 48%, respectively lower in mice treated with DOXO alone than in mice treated with DOXO plus EMPA. Similar findings were obtained in kidney tissue extract, i.e., IL-1β, IL-6 and IL-8 expression was 29.5%, 41% and 47% lower in mice treated with DOXO plus EMPA than in mice treated with DOXO alone (*Figure 4, A*). The use of EMPA reduces the magnitude of cardiac effects, decreasing significantly the expression of MyD88 and NLRP3 by 35-40 % ($p <0.001$) (*Figure 4, B*).

Moreover, cardiac collagen (in red in histological pictures in *Figure 5 A*, and expressed as percentage of tissue area in *Figure 5 B*), was significantly greater in mice treated with DOXO versus untreated mice ($p<0.005$). Apoptotic nuclei in cardiac tissue (see green signals in *Figure 5 C*) were 15.8-fold more numerous in DOXO-treated than in untreated mice, and the number of apoptotic events was 35% lower in EMPA-treated mice than in DOXO-treated mice($p<0.001$), which indicates that EMPA exerts a cardioprotective effect *in vivo.* Apoptosis was clearly lower (green signal in *Figure 5 C*) in mice treated with EMPA/DOXO compared to DOXO alone, in line with quantitative data shown in *Figure 5 D*.

We calculated the strain on long-axis images and ventricular function is studied by myocardial deformation along the radial and longitudinal axes, as useful echocardiographic markers of cardiotoxicity [38,39,40,41]. Strain analysis showed that EMPA significantly improves cardiac function when used in combination with DOXO compared to DOXO treated mice. Radial strain (RS) is 30.3 % in EMPA-DOXO vs 15.7% in DOXO groups ($P<0.001$) ; longitudinal strain (LS) is -17% in EMPA-DOXO vs -11,7% in DOXO groups ($P<0.001$) (*Figure 6*). Moreover, the association of EMPA and DOXO brings strain levels similar to those of untreated mice (control) (*Figure 6*), clearly indicating a cardioprotective effect of EMPA in DOXO-induced cardiotoxicity.

Discussion

In patients with type 2 diabetes and established cardiovascular disease, empagliflozin reduced the risk of cardiovascular death and heart failure hospitalizations in the EMPA-REG OUTCOME® trial [8,9]. More recently, empagliflozin reduced heart failure hospitalizations and cardiovascular mortality in both high and low risk patients thereby confirming its robust and significant cardioprotective effects [42].

DOXO-induced cardiotoxicity is induced by several mechanisms mediated by increased levels of iROS and $[Ca^{2+}]i$ in cardiomyocytes associated to a pro-inflammatory cytokine storm leading to apoptosis, necrosis and mitochondrial dysfunctions. Moreover, treatment with doxorubicin leading to a systemic and local inflammation in cancer patients, partially due to cytosolic damages several organs like liver and heart; doxorubicin exposure in liver increased the production of circulating IL-1-β, IL-6 and hs-CRP (hypersensitive-C-reactive-protein) leading to increased risk of cardiovascular and metabolic diseases [43]. Other preclinical and clinical studies evidenced direct damages induced by doxorubicin, partially mediated by reduced AMPK expression and induction of double-strand breaks and cell death by intercalating into DNA and blocking the activity of the topoisomerase II (TOP2) enzymes called TOP2β and TOP2α [44]. Therefore, consolidated that empagliflozin exerts systemic and cardiac anti-inflammatory effects in preclinical and clinical trials, its use during treatment with doxorubicin is a promising cardioprotective strategy.

A recent preclinical study suggests that empagliflozin could reduce intracellular Ca^{2+} under high glucose [45]. It is feasible that empagliflozin exerts this effect by inhibiting the Na^{+}/H^{+} exchanger, thereby leading to a lower concentration of intracellular Ca^{2+} in cardiomyocytes [46,47]. Given that DOXO exerts cardiotoxic effects by increasing intracellular Ca^{2+}concentration [47,48] it is feasible that the improvement of calcium homeostasis contributes to the cardioprotective effects of empagliflozin and cardiomyocyte contractility.

Recent preclinical and clinical studies demonstrated that oxidative stress is one of the most important events implicated in the cardiotoxicity of anticancer drugs [49]. Interestingly, empagliflozin exerts antioxidant effects in cardiomyocytes thereby reducing lipid peroxidation during incubation with DOXO [50,51,52]. Notably, NO is over-produced in anthracycline-treated patients [53] thereby increasing the risk of cardiac failure and cardiomyopathy [54].Our finding that empagliflozin reduces NO production in cells exposed to DOXO lays the preliminary foundation for preclinical studies of NO homeostasis in cancer patients.

The pro-inflammatory heart microenvironment is a key driving force of the cardiotoxicity seen in cancer patients [55,56,57]. The pharmacological inhibition of IL-1 improves the left ventricle ejection fraction and fraction shortening in preclinical models during DOXO exposure [58]. Interleukins 8 and 6 are also associated to cardiovascular disease, heart failure and stroke [59]. Here, empagliflozin improved cardiac, hepatic and renal microenvironment through the reduction of pro-inflammatory cytokines during treatment with DOXO.As summarized in Figure 7, empagliflozin inhibits activity of SGLT-2 thereby reducing intracellular glucose and sodium in cardiomyocytes, consequently increasing 5' AMP-activated protein kinase (AMPK) that has a key role in doxorubicin-mediated cardiomyocyte injury through SMAD,

NoX and Wnt [60]. The overall picture of the study is in line with other recent work highlighting on the protective effects of SGLT2 inhibitors on DOXO induced cardiotoxicity [61,62].

Concentration and administration time of DOXO were in agree with other previous preclinical studies of anthracycline-induced cardiotoxicity [23, 63]; more in details, mice analysed through echocardiography after 10 days of treatment with DOXO to measure left ventricular systolic function, heart rate and cardiac output, were previously described [63,64] and in accordance to the recommendations of the American Society of Echocardiography [65].

Study limitations

Unfortunately, we have not quantified circulating Troponin-T and BNP levels in mice due to unavailability of the kits, however further studies will be performed in order to analyze the effect of empagliflozin on circulating markers of cardiac damages during treatment with cardiotoxic drugs. Effects of empagliflozin treatment on glucose levels in mice were not studied; however, several studies clearly demonstrated that SGLT-2 inhibitors administration to nondiabetic patients significantly improves LV volumes, LV mass, LV systolic function, functional capacity, and quality of life when compared with placebo, independently of their glycemic status [67,68].

Clinical Perspective

Currently, there is the lack of the safe cardioprotective drug against doxorubicin without any effect on cancer treatment or incidence of secondary cancers. We believe that the effects of empagliflozin on the radial and longitudinal strain seen in preclinical models after treatment with doxorubicin may be of useful clinical significance in the primary prevention of heart damage from anthracycline treatment. Given the well-known higher cumulative incidence of heart failure and cardiomyopathy seen in older woman treated with anthracyclines and the anti-HER2 antibody trastuzumab, compared to the single treatments, during first three years after diagnosis by cancer therapy [69] , we are planning to conduct preclinical studies to evaluate whether empagliflozin could have cardioprotective properties against this combination therapy, considering that same mechanisms of trastuzumab-induced cardiotoxicity involves pro-inflammatory and pro-oxidative pathways [70].

Conclusion

The present study identified the mechanism whereby empagliflozin exerts anti-inflammatory and cardioprotective effects in DOXO-induced cardiotoxicity, thereby providing a new therapeutic option for patients undergoing anthracycline-based therapy. The cardioprotective effects of EMPA are biochemically explained by an improvement of the myocardial pro-inflammatory microenvironment and a reduced pro-oxidative state. This study provides the proof of concept for translational studies designed to investigate the cardioprotective use of empagliflozin during treatments with doxorubicin in cancer patients.

Abbreviations

DOXO: Doxorubicin

DOXO + EMPA: Doxorubicin plus empagliflozin

LV: Left ventricular

EF: Ejection fraction

LS: Longitudinal strain

EMPA: Empagliflozin

SGLT2: Selective inhibitor of the sodium glucose co-transporter 2

FS: Fractional shortening

SD: Standard deviations

RS: Radial strain

NHE: Na+/H+ exchanger

iROS: Intracellular Reactive oxygen species

MDA: Malondialdehyde

4HNA: 4-hydroxy-nonenoic acid

NLRP3: NOD-, LRR- and pyrin domain-containing protein 3

MyD88: Myddosome type 88

Declarations

Ethics approval and consent to participate: Not applicable

Consent for publication: Not applicable.

Availability of data and materials: The data used and/or analysed during the current study are available from the corresponding author on reasonable request.

Competing interests : All the authors declare no conflict of interests.

Funding: This work was funded by an “Ricerca Corrente” grant from the Italian Ministry of Health.

Authors' contributions: N.M and V.Q came up with the research idea, study design, and concept. V.Q., A.B., A.C, D.R., and G.M. performed experiments. G.B. and N.M . analysed and interpreted data. V.Q., D.R., and

N.M wrote the manuscript and the other authors critically reviewed it. M.D and NM. supervised all aspects of this study, including design, execution, and interpretation of the data.

Acknowledgements: The authors thank Jean Ann Gilder (Scientific Communication srl., Naples, Italy) for language editing.

References

1. Baxter-Holland M, Dass CR. Doxorubicin, mesenchymal stem cell toxicity and antitumour activity: implications for clinical use. J Pharm Pharmacol. 2018 Mar;70(3):320-327. doi: 10.1111/jphp.12869. Epub 2018 Jan 22.
2. Mascarenhas L, Malogolowkin M, Armenian SH, Sposto R, Venkatramani R. A phase I study of oxaliplatin and doxorubicin in pediatric patients with relapsed or refractory extracranial non-hematopoietic solid tumors.Pediatr Blood Cancer. 2013 Jul;60(7):1103-7. doi: 10.1002/pbc.24471. Epub 2013 Jan 17.
3. Khouri MG, Douglas PS, Mackey JR, Martin M, Scott JM, Scherrer-Crosbie M, Jones LW. Cancer therapy-induced cardiac toxicity in early breast cancer: addressing the unresolved issues. Circulation 2012;126:2749–276
4. Mele D, Tocchetti CG, Pagliaro P, Madonna R, Novo G, Pepe A, Zito C, Maurea N, Spallarossa P Pathophysiology of anthracycline cardiotoxicity. J Cardiovasc Med (Hagerstown). 2016 May; 17 Suppl 1 Special issue on Cardiotoxicity from Antiblastic Drugs and Cardioprotection():e3-e11.
5. Rea D, Coppola C, Barbieri A, Monti MG, Misso G, Palma G, Bimonte S, Zarone MR, Luciano A, Liccardo D, Maiolino P, Cittadini A, Ciliberto G, Arra C, Maurea N. Strain Analysis in the Assessment of a Mouse Model of Cardiotoxicity due to Chemotherapy: Sample for Preclinical Research. In Vivo. 2016 May-Jun;30(3):279-90.
6. White JR Jr.Empagliflozin, an SGLT2 inhibitor for the treatment of type 2 diabetes mellitus: a review of the evidence. Ann Pharmacother. 2015 May;49(5):582-98. doi: 10.1177/1060028015573564. Epub 2015 Feb 23. Review.
7. Muscelli E, Astiarraga B, Barsotti E, Mari A, Schliess F, Nosek L, Heise T, Broedl UC, Woerle HJ, Ferrannini E. Metabolic consequences of acute and chronic empagliflozin administration in treatment-naive and metformin pretreated patients with type 2 diabetes. Diabetologia. 2016 Apr;59(4):700-8. doi: 10.1007/s00125-015-3845-8. Epub 2015 Dec 24.
8. Zinman B, Wanner C, Lachin JM, Fitchett D, Bluhmki E, Hantel S, Mattheus M, Devins T, Johansen OE, Woerle HJ, Broedl UC, Inzucchi SE; EMPA-REG OUTCOME Investigators. Empagliflozin, Cardiovascular Outcomes, and Mortality in Type 2 Diabetes. N Engl J Med. 2015 Nov 26;373(22):2117-28. doi: 10.1056/NEJMoa1504720. Epub 2015 Sep 17.
9. Zinman B, Inzucchi SE2, Wanner C3, Hehnke U4, George JT4, Johansen OE5, Fitchett D6; EMPA-REG OUTCOME® investigators. Empagliflozin in women with type 2 diabetes and cardiovascular disease -

an analysis of EMPA-REG OUTCOME®. Diabetologia. 2018 Jul;61(7):1522-1527. doi: 10.1007/s00125-018-4630-2. Epub 2018 Apr 30.

10. Cavero-Redondo I, Peleteiro B, Álvarez-Bueno C, Rodriguez-Artalejo F, Martínez-Vizcaíno V. Glycated haemoglobin A1c as a risk factor of cardiovascular outcomes and all-cause mortality in diabetic and non-diabetic populations: a systematic review and meta-analysis. BMJ Open. 2017 Jul 31;7(7):e015949. doi: 10.1136/bmjopen-2017-015949.
11. Packer M, Anker SD, Butler J, Filippatos G, Pocock SJ, Carson P, Januzzi J, Verma S, Tsutsui H, Brueckmann M, Jamal W, Kimura K, Schnee J, Zeller C, Cotton D, Bocchi E, Böhm M, Choi DJ, Chopra V, Chuquiure E, Giannetti N, Janssens S, Zhang J, Gonzalez Juanatey JR, Kaul S, Brunner-La Rocca HP, Merkely B, Nicholls SJ, Perrone S, Pina I, Ponikowski P, Sattar N, Senni M, Seronde MF, Spinar J, Squire I, Taddei S, Wanner C, Zannad F; EMPEROR-Reduced Trial Investigators. Cardiovascular and Renal Outcomes with Empagliflozin in Heart Failure. N Engl J Med. 2020 Aug 29. doi: 10.1056/NEJMoa2022190. Epub ahead of print. PMID: 32865377.
12. Quagliariello V, Vecchione R, Coppola C, Di Cicco C, De Capua A, Piscopo G, Paciello R, Narciso V, Formisano C, Taglialatela-Scafati O, Iaffaioli RV, Botti G, Netti PA, Maurea N. Cardioprotective Effects of Nanoemulsions Loaded with Anti-Inflammatory Nutraceuticals against Doxorubicin-Induced Cardiotoxicity. Nutrients. 2018 Sep 14;10(9). pii: E1304. doi: 10.3390/nu10091304.
13. Barbarisi M, Iaffaioli RV, Armenia E, Schiavo L, De Sena G, Tafuto S, Barbarisi A, Quagliariello V. Novel nanohydrogel of hyaluronic acid loaded with quercetin alone and in combination with temozolomide as new therapeutic tool, CD44 targeted based, of glioblastoma multiforme. J Cell Physiol. 2018 Oct;233(10):6550-6564. doi: 10.1002/jcp.26238. Epub 2018 May 8.
14. Darrabie MD, Arciniegas AJ, Mantilla JG, Mishra R, Vera MP, Santacruz L, Jacobs DO. Exposing cardiomyocytes to subclinical concentrations of doxorubicin rapidly reduces their creatine transport. Am J Physiol Heart Circ Physiol. 2012 Sep 1;303(5):H539-48. doi: 10.1152/ajpheart.00108.2012
15. Greene RF , Collins JM , Jenkins JF , Speyer JL , Myers CE . Plasma pharmacokinetics of adriamycin and adriamycinol: implications for the design of in vitro experiments and treatment protocols. Cancer Res 43: 3417–3421, 1983.
16. Quagliariello V, Iaffaioli RV, Armenia E, Clemente O, Barbarisi M, Nasti G, Berretta M, Ottaiano A, Barbarisi A. Hyaluronic Acid Nanohydrogel Loaded With Quercetin Alone or in Combination to a Macrolide Derivative of Rapamycin RAD001 (Everolimus) as a New Treatment for Hormone-Responsive Human Breast Cancer. J Cell Physiol. 2017 Aug; 232(8):2063-2074.
17. Mele D, Tocchetti CG, Pagliaro P, Madonna R, Novo G, Pepe A, Zito C, Maurea N, Spallarossa P. Pathophysiology of anthracycline cardiotoxicity. J Cardiovasc Med (Hagerstown). 2016 May;17 Suppl 1 Special issue on Cardiotoxicity from Antiblastic Drugs and Cardioprotection:e3-e11. Review.
18. Kim H, Park GS, Lee JE, Kim JH. A leukotriene B4 receptor-2 is associated with paclitaxel resistance in MCF-7/DOX breast cancer cells. Br J Cancer. 2013 Jul 23;109(2):351-9. doi: 10.1038/bjc.2013.333. Epub 2013 Jun 25.

19. Nakabayashi H, Shimizu K. Involvement of Akt/NF-κB pathway in antitumor effects of parthenolide on glioblastoma cells in vitro and in vivo. BMC Cancer. 2012 Oct 5;12:453. doi: 10.1186/1471-2407-12-453.
20. Di Stadio CS, Altieri F, Miselli G, Elce A, Severino V, Chambery A, Quagliariello V, Villano V, de Dominicis G, Rippa E, Arcari P. AMP18 interacts with the anion exchanger SLC26A3 and enhances its expression in gastric cancer cells. Biochimie. 2016 Feb;121:151-60. doi: 10.1016/j.biochi.2015.12.010. Epub 2015 Dec 15.
21. Tocchetti CG, Carpi A, Coppola C, Quintavalle C, Rea D, Campesan M, Arcari A, Piscopo G, Cipresso C, Monti MG, De Lorenzo C, Arra C, Condorelli G, Di Lisa F, Maurea N. Ranolazine protects from doxorubicin-induced oxidative stress and cardiac dysfunction. Eur J Heart Fail. 2014 Apr;16(4):358-66. doi: 10.1002/ejhf.50. PMID: 24464789
22. Coppola C, Riccio G, Barbieri A, Monti MG, Piscopo G, Rea D, Arra C, Maurea C, De Lorenzo C, Maurea N. Antineoplastic-related cardiotoxicity, morphofunctional aspects in a murine model: contribution of the new tool 2D-speckle tracking. Onco Targets Ther. 2016 Nov 2;9:6785-6794. doi: 10.2147/OTT.S106528. PMID: 27843329; PMCID: PMC5098586.
23. Fedele C, Riccio G, Coppola C, Barbieri A, Monti MG, Arra C, Tocchetti CG, D'Alessio G, Maurea N, De Lorenzo C. Comparison of preclinical cardiotoxic effects of different ErbB2 inhibitors. Breast Cancer Res Treat. 2012 Jun;133(2):511-21. doi: 10.1007/s10549-011-1783-9. Epub 2011 Sep 27. PMID: 21947749.
24. Riccio G, Antonucci S, Coppola C, D'Avino C, Piscopo G, Fiore D, Maurea C, Russo M, Rea D, Arra C, Condorelli G, Di Lisa F, Tocchetti CG, De Lorenzo C, Maurea N. Ranolazine Attenuates Trastuzumab-Induced Heart Dysfunction by Modulating ROS Production. Front Physiol. 2018 Feb 6;9:38. doi: 10.3389/fphys.2018.00038. eCollection 2018.
25. Pistner A, Belmonte S, Coulthard T, Blaxall B. Murine echocardiography and ultrasound imaging. J Vis Exp. 2010 Aug 8;(42):2100. doi: 10.3791/2100. PMID: 20736912; PMCID: PMC3156019.
26. Tee N, Gu Y, Murni, Shim W. Comparative myocardial deformation in 3 myocardial layers in mice by speckle tracking echocardiography. Biomed Res Int. 2015;2015:148501. doi: 10.1155/2015/148501. Epub 2015 Mar 2. PMID: 25821784; PMCID: PMC4363535.
27. Donner DG, Kiriazis H, Du XJ, Marwick TH, McMullen JR. Improving the quality of preclinical research echocardiography: observations, training, and guidelines for measurement. Am J Physiol Heart Circ Physiol. 2018 Jul 1;315(1):H58-H70. doi: 10.1152/ajpheart.00157.2018. Epub 2018 Apr 20. PMID: 29677464.
28. de Lucia C, Wallner M, Eaton DM, Zhao H, Houser SR, Koch WJ. Echocardiographic Strain Analysis for the Early Detection of Left Ventricular Systolic/Diastolic Dysfunction and Dyssynchrony in a Mouse Model of Physiological Aging. J Gerontol A Biol Sci Med Sci. 2019 Mar 14;74(4):455-461. doi: 10.1093/gerona/gly139. PMID: 29917053; PMCID: PMC6417453.
29. https://www.biotech.cornell.edu/sites/default/files/202006/Vevo%202100%20Echocardiography.pdf

30. Sabatino J, De Rosa S, Tammè L, Iaconetti C, Sorrentino S, Polimeni A, Mignogna C, Amorosi A, Spaccarotella C, Yasuda M, Indolfi C. Empagliflozin prevents doxorubicin-induced myocardial dysfunction. Cardiovasc Diabetol. 2020 May 15;19(1):66. doi: 10.1186/s12933-020-01040-5. PMID: 32414364; PMCID: PMC7229599.
31. Eliaa SG, Al-Karmalawy AA, Saleh RM, Elshal MF. Empagliflozin and Doxorubicin Synergistically Inhibit the Survival of Triple-Negative Breast Cancer Cells via Interfering with the mTOR Pathway and Inhibition of Calmodulin: In Vitro and Molecular Docking Studies. ACS Pharmacol Transl Sci. 2020 Nov 11;3(6):1330-1338. doi: 10.1021/acsptsci.0c00144. PMID: 33344906; PMCID: PMC7737321.
32. Sayed-Ahmed MM, Khattab MM, Gad MZ, Osman AM. Increased plasma endothelin-1 and cardiac nitric oxide during doxorubicin-induced cardiomyopathy. PharmacolToxicol. 2001 Sep; 89(3):140-4.
33. Aldieri E, Bergandi L, Riganti C, Costamagna C, Bosia A, Ghigo D. Doxorubicin induces an increase of nitric oxide synthesis in rat cardiac cells that is inhibited by iron supplementation. ToxicolApplPharmacol. 2002 Dec 1; 185(2):85-90.
34. Quagliariello V, Vecchione R, Coppola C, Di Cicco C, De Capua A, Piscopo G, Paciello R, Narciso V, Formisano C, Taglialatela-Scafati O, Iaffaioli RV, Botti G, Netti PA, Maurea N. Cardioprotective Effects of Nanoemulsions Loaded with Anti-Inflammatory Nutraceuticals against Doxorubicin-Induced Cardiotoxicity. Nutrients. 2018 Sep 14;10(9). pii: E1304. doi: 10.3390/nu10091304.
35. Bacchiega BC, Bacchiega AB, Usnayo MJ, Bedirian R, Singh G, Pinheiro GD. Interleukin 6 Inhibition and Coronary Artery Disease in a High-Risk Population: A Prospective Community-Based Clinical Study. J Am Heart Assoc. 2017 Mar 13;6(3). pii: e005038. doi: 10.1161/JAHA.116.005038.
36. Pecoraro M, Del Pizzo M, Marzocco S, Sorrentino R, Ciccarelli M, Iaccarino G, Pinto A, Popolo A. Inflammatory mediators in a short-time mouse model of doxorubicin-induced cardiotoxicity. 2016 Feb 15;293:44-52. doi: 10.1016/j.taap.2016.01.006. Epub 2016 Jan 11.
37. Andreadou I, Efentakis P, Balafas E, Togliatto G, Davos CH, Varela A, Dimitriou CA, Nikolaou PE, Maratou E, Lambadiari V, Ikonomidis I, Kostomitsopoulos N, Brizzi MF, Dimitriadis G, Iliodromitis EK. Empagliflozin Limits Myocardial Infarction in Vivo and Cell Death in Vitro: Role of STAT3, Mitochondria, and Redox Aspects.Front Physiol. 2017 Dec 19;8:1077. doi: 10.3389/fphys.2017.01077. eCollection 2017.
38. Arciniegas Calle MC, Sandhu NP, Xia H, Cha SS, Pellikka PA, Ye Z, Herrmann J, Villarraga HR. Two-dimensional speckle tracking echocardiography predicts early subclinical cardiotoxicity associated with anthracycline-trastuzumab chemotherapy in patients with breast cancer. BMC Cancer. 2018 Oct 25;18(1):1037. doi: 10.1186/s12885-018-4935-z.
39. Sawaya H, Sebag IA, Plana JC, Januzzi JL, Ky B, Tan TC, Cohen V, Banchs J, Carver JR, Wiegers SE, Martin RP, Picard MH, Gerszten RE, Halpern EF, Passeri J, Kuter I, Scherrer-Crosbie M.H Sawaya, IA Sebag, JC Plana, JL Januzzi, B Ky, V Cohen, S Gosavi, JR Carver, SE Wiegers, RP Martin, MH Picard, RE Gerszten, EF Halpern, J Passeri, I Kuter, M Scherrer-Crosbie. Assessment of echocardiography and biomarkers for the extended prediction of cardiotoxicity in patients treated with anthracyclines, taxanes, and trastuzumab. Circ Cardiovasc Imaging. 2012 Sep 1;5(5):596-603.

40. Early detection and prediction of cardiotoxicity in chemotherapy-treated patients. Am J Cardiol, 107 (2011), pp. 1375-1380
41. Sawaya H1, Sebag IA, Plana JC, Januzzi JL, Ky B, Tan TC, Cohen V, Banchs J, Carver JR, Wiegers SE, Martin RP, Picard MH, Gerszten RE, Halpern EF, Passeri J, Kuter I, Scherrer-Crosbie M. Assessment of echocardiography and biomarkers for the extended prediction of cardiotoxicity in patients treated with anthracyclines, taxanes, and trastuzumab. Circ Cardiovasc Imaging. 2012 Sep 1;5(5):596-603. Epub 2012 Jun 28.
42. Fitchett D, Butler J, van de Borne P, Zinman B, Lachin JM, Wanner C, Woerle HJ, Hantel S, George JT, Johansen OE, Inzucchi SE; EMPA-REG OUTCOME® trial investigators. Effects of empagliflozin on risk for cardiovascular death and heart failure hospitalization across the spectrum of heart failure risk in the EMPA-REG OUTCOME® trial. Eur Heart J. 2018 Feb 1;39(5):363-370. doi: 10.1093/eurheartj/ehx511.
43. Wang L, Chen Q, Qi H, Wang C, Wang C, Zhang J, Dong L. Doxorubicin-Induced Systemic Inflammation Is Driven by Upregulation of Toll-Like Receptor TLR4 and Endotoxin Leakage. Cancer Res. 2016 Nov 15;76(22):6631-6642. doi: 10.1158/0008-5472.CAN-15-3034. Epub 2016 Sep 28. PMID: 27680684.
44. yu YL, Kerrigan JE, Lin CP, Azarova AM, Tsai YC, Ban Y, Liu LF. Topoisomerase IIbeta mediated DNA double-strand breaks: implications in doxorubicin cardiotoxicity and prevention by dexrazoxane. Cancer Res. 2007 Sep 15;67(18):8839-46. doi: 10.1158/0008-5472.CAN-07-1649. PMID: 17875725.
45. Ng KM, Lau YM, Dhandhania V, Cai ZJ, Lee YK, Lai WH, Tse HF, Siu C. Empagliflozin Ammeliorates High Glucose Induced-Cardiac Dysfuntion in Human iPSC-Derived Cardiomyocytes. Sci Rep. 2018 Oct 5;8(1):14872. doi: 10.1038/s41598-018-33293-2.
46. Baartscheer A, Schumacher CA, Wust RC, Fiolet JW, Stienen GJ, Coronel R, Zuurbier CJ. Empagliflozin decreases myocardial cytoplasmic Na+ through inhibition of the cardiac Na+/H+ exchanger in rats and rabbits. Diabetologia2017;60:568–573.
47. Mele D, Tocchetti CG, Pagliaro P, Madonna R, Novo G, Pepe A, Zito C, Maurea N, Spallarossa P. Pathophysiology of anthracycline cardiotoxicity. J Cardiovasc Med (Hagerstown). 2016 May;17 Suppl1:S3-S11. doi: 10.2459/JCM.0000000000000378. Review.
48. Quagliariello V, Vecchione R, Coppola C, Di Cicco C, De Capua A, Piscopo G, Paciello R, Narciso V, Formisano C, Taglialatela-Scafati O, Iaffaioli RV, Botti G, Netti PA, Maurea N. Cardioprotective Effects of Nanoemulsions Loaded with Anti-Inflammatory Nutraceuticals against Doxorubicin-Induced Cardiotoxicity. Nutrients. 2018 Sep 14;10(9). pii: E1304. doi: 10.3390/nu10091304.
49. Hrelia S, Fiorentini D, Maraldi T, Angeloni C, Bordoni A, Biagi PL, Hakim G. Doxorubicin induces early lipid peroxidation associated with changes in glucose transport in cultured cardiomyocytes. BiochimBiophysActa. 2002 Dec 23;1567(1-2):150-6.
50. Li C, Zhang J, Xue M, Li X, Han F, Liu X, Xu L, Lu Y, Cheng Y, Li T, Yu X, Sun B, Chen L.SGLT2 inhibition with empagliflozin attenuates myocardial oxidative stress and fibrosis in diabetic mice heart. CardiovascDiabetol. 2019 Feb 2;18(1):15. doi: 10.1186/s12933-019-0816-2.

51. Pabel S, Wagner S, Bollenberg H, Bengel P, Kovács Á, Schach C, Tirilomis P, Mustroph J, Renner A, Gummert J, Fischer T, Van Linthout S, Tschöpe C, Streckfuss-Bömeke K, Hasenfuss G, Maier LS, Hamdani N, Sossalla S. Empagliflozin directly improves diastolic function in human heart failure. Eur J Heart Fail. 2018 Dec;20(12):1690-1700. doi: 10.1002/ejhf.1328. Epub 2018 Oct 17.
52. Octavia Y, Tocchetti CG, Gabrielson KL, Janssens S, Crijns HJ, Moens AL. Doxorubicin-induced cardiomyopathy: from molecular mechanisms to therapeutic strategies. J Mol Cell Cardiol. 2012 Jun;52(6):1213-25. doi: 10.1016/j.yjmcc.2012.03.006. Epub 2012 Mar 21.
53. Guerra J, De Jesus A, Santiago-Borrero P, Roman-Franco A, Rodríguez E, Crespo MJ. Plasma nitric oxide levels used as an indicator of doxorubicin-induced cardiotoxicity in rats. Hematol J. 2005; 5(7):584-8.
54. Kalivendi SV, Kotamraju S, Zhao H, Joseph J, Kalyanaraman B. Doxorubicin-induced apoptosis is associated with increased transcription of endothelial nitric-oxide synthase. Effect of antiapoptotic antioxidants and calcium. J Biol Chem. 2001 Dec 14; 276(50):47266-76.
55. Han X, Zhou Y, Liu W. Precision cardio-oncology: understanding the cardiotoxicity of cancer therapy. NPJ Precis Oncol. 2017 Sep 12;1(1):31. doi: 10.1038/s41698-017-0034-x. eCollection 2017.Biomed Pharmacother. 2011 Oct;65(7):481-5. doi: 10.1016/j.biopha.2011.06.005. Epub 2011 Aug 27.
56. Zhu J, Zhang J, Zhang L, Du R, Xiang D, Wu M, Zhang R, Han W.Interleukin-1 signaling mediates acute doxorubicin-induced cardiotoxicity.
57. Sauter KA, Wood LJ, Wong J, Iordanov M, Magun BE. Doxorubicin and daunorubicin induce processing and release of interleukin-1β through activation of the NLRP3 inflammasome.Cancer BiolTher. 2011 Jun 15;11(12):1008-16. Epub 2011 Jun 15.
58. Zhu J, Zhang J, Xiang D, Zhang Z, Zhang L, Wu M, Zhu S, Zhang R, Han W. Recombinant human interleukin-1 receptor antagonist protects mice against acute doxorubicin-induced cardiotoxicity. Eur J Pharmacol. 2010 Sep 25; 643(2-3):247-53.
59. Apostolakis S, Vogiatzi K, Amanatidou V, Spandidos DA. Cardiovasc Res. 2009 Dec 1;84(3):353-60. doi: 10.1093/cvr/cvp241. Epub 2009 Jul 18. Interleukin 8 and cardiovascular disease.
60. Timm KN, Tyler DJ. The Role of AMPK Activation for Cardioprotection in Doxorubicin-Induced Cardiotoxicity. Cardiovasc Drugs Ther. 2020 Apr;34(2):255-269. doi: 10.1007/s10557-020-06941-x. PMID: 32034646; PMCID: PMC7125062.
61. Oh CM, Cho S, Jang JY, Kim H, Chun S, Choi M, Park S, Ko YG. Cardioprotective Potential of an SGLT2 Inhibitor Against Doxorubicin-Induced Heart Failure. Korean Circ J. 2019 Dec;49(12):1183-1195. doi: 10.4070/kcj.2019.0180. Epub 2019 Jul 31. PMID: 31456369; PMCID: PMC6875592.
62. Yang CC, Chen YT, Wallace CG, Chen KH, Cheng BC, Sung PH, Li YC, Ko SF, Chang HW, Yip HK. Early administration of empagliflozin preserved heart function in cardiorenal syndrome in rat. Biomed Pharmacother. 2019 Jan;109:658-670. doi: 10.1016/j.biopha.2018.10.095. Epub 2018 Nov 4. PMID: 30404073.
63. Toldo S, Goehe RW, Lotrionte M, Mezzaroma E, Sumner ET, Biondi-Zoccai GG, Seropian IM, Van Tassell BW, Loperfido F, Palazzoni G, Voelkel NF, Abbate A, Gewirtz DA. Comparative cardiac toxicity

of anthracyclines in vitro and in vivo in the mouse. PLoS One. 2013;8(3):e58421. doi:

64. Toldo S, Bogaard HJ, Van Tassell BW, Mezzaroma E, Seropian IM, et al. (2011) Right ventricular dysfunction following acute myocardial infarction in the absence of pulmonary hypertension in the mouse. PLoS One 6: e18102.
65. Gardin JM, Adams DB, Douglas PS, Feigenbaum H, Forst DH, et al. (2002) Recommendations for a standardized report for adult transthoracic echocardiography: a report from the American Society of Echocardiography's Nomenclature and Standards Committee and Task Force for a Standardized Echocardiography Report. J Am Soc Echocardiogr 15: 275–90.
66. Romera I, Ampudia-Blasco FJ, Pérez A, Ariño B, Pfarr E, Giljanovic Kis S, Naderali E. Efficacy and safety of empagliflozin in combination with other oral hypoglycemic agents in patients with type 2 diabetes mellitus. Endocrinol Nutr. 2016 Dec;63(10):519-526. English, Spanish. doi: 10.1016/j.endonu.2016.06.003. Epub 2016 Aug 28. PMID: 27578024.
67. Dekkers CCJ, Gansevoort RT. Sodium-glucose cotransporter 2 inhibitors: extending the indication to non-diabetic kidney disease? Nephrol Dial Transplant. 2020 Jan 1;35(Suppl 1):i33-i42. doi: 10.1093/ndt/gfz264. PMID: 32003836; PMCID: PMC6993196.
68. Santos-Gallego CG, Vargas-Delgado AP, Requena-Ibanez JA, Garcia-Ropero A, Mancini D, Pinney S, Macaluso F, Sartori S, Roque M, Sabatel-Perez F, Rodriguez-Cordero A, Zafar MU, Fergus I, Atallah-Lajam F, Contreras JP, Varley C, Moreno PR, Abascal VM, Lala A, Tamler R, Sanz J, Fuster V, Badimon JJ; EMPA-TROPISM (ATRU-4) Investigators. Randomized Trial of Empagliflozin in Nondiabetic Patients With Heart Failure and Reduced Ejection Fraction. J Am Coll Cardiol. 2021 Jan 26;77(3):243-255. doi: 1016/j.jacc.2020.11.008. Epub 2020 Nov 13. PMID: 33197559.
69. Chen J, Long JB, Hurria A, Owusu C, Steingart RM, Gross CP. Incidence of heart failure or cardiomyopathy after adjuvant trastuzumab therapy for breast cancer. J Am Coll Cardiol. 2012 Dec 18;60(24):2504-12. doi: 10.1016/j.jacc.2012.07.068. Epub 2012 Nov 14.
70. Maurea N, Coppola C, Piscopo G, Galletta F, Riccio G, Esposito E, De Lorenzo C, De Laurentiis M, Spallarossa P, Mercuro G. Pathophysiology of cardiotoxicity from target therapy and angiogenesis inhibitors. J Cardiovasc Med (Hagerstown). 2016 May;17 Suppl 1 Special issue on Cardiotoxicity from Antiblastic Drugs and Cardioprotection:e19-e26.

Figures

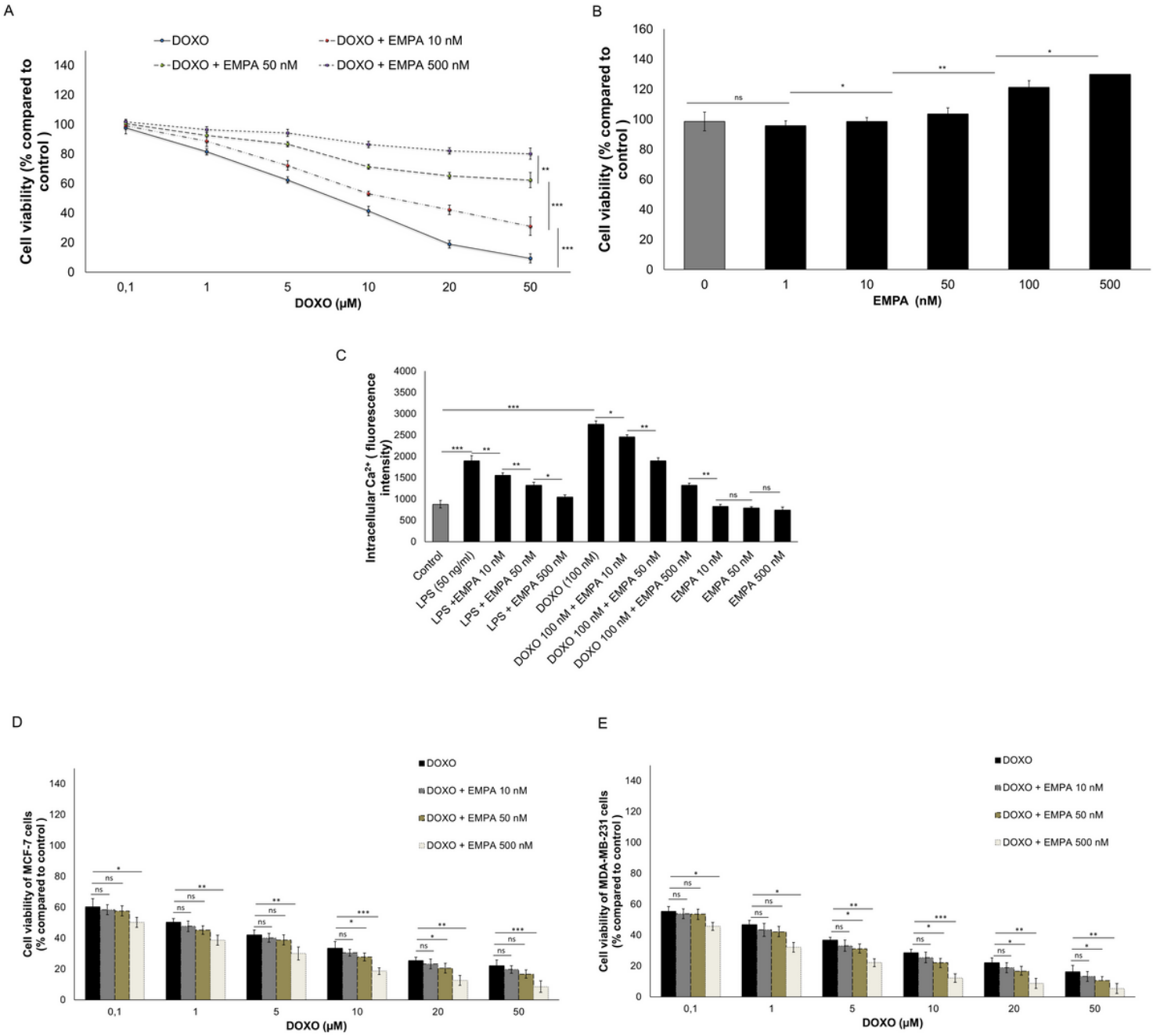

Figure 1

EMPA exerts a cytoprotective effect on cardiomyocytes exposed to doxorubicin (DOXO) through the reduction of intracellular Ca2+ overload in a concentration-dependent manner. 10 x103 HL-1 cells/well were seeded in 96-well plate and were cultured under different conditions. (A) cell viability of cardiomyocytes treated with DOXO (from 0.1 to 50 µM), alone or combined with empagliflozin (EMPA) (10, 50 or 500 nM) (n=6 for each concentration. One-way ANOVA analysis) (B) Cardiomyocyte viability under exposure to EMPA from 1 to 500 nM. (n=6 for each concentration. One-way ANOVA analysis). (C) For quantification of intracellular calcium (Ca2+), 5x103 cells/well were seeded in a 24-well plate and allowed to grow for 24 hours; after, cardiomyocytes were not exposed (control) or exposed to EMPA (10, 50, 500 nM), lipopolysaccharides (LPS) (50 ng/ml) or DOXO (100 nM) alone or with EMPA at 10, 50 and

500 nM. (n=3 for each group). One-way ANOVA analysis). Values are expressed ± SD. ***P<0.001; **P<0.01; *P<0.05; ns: not significant.

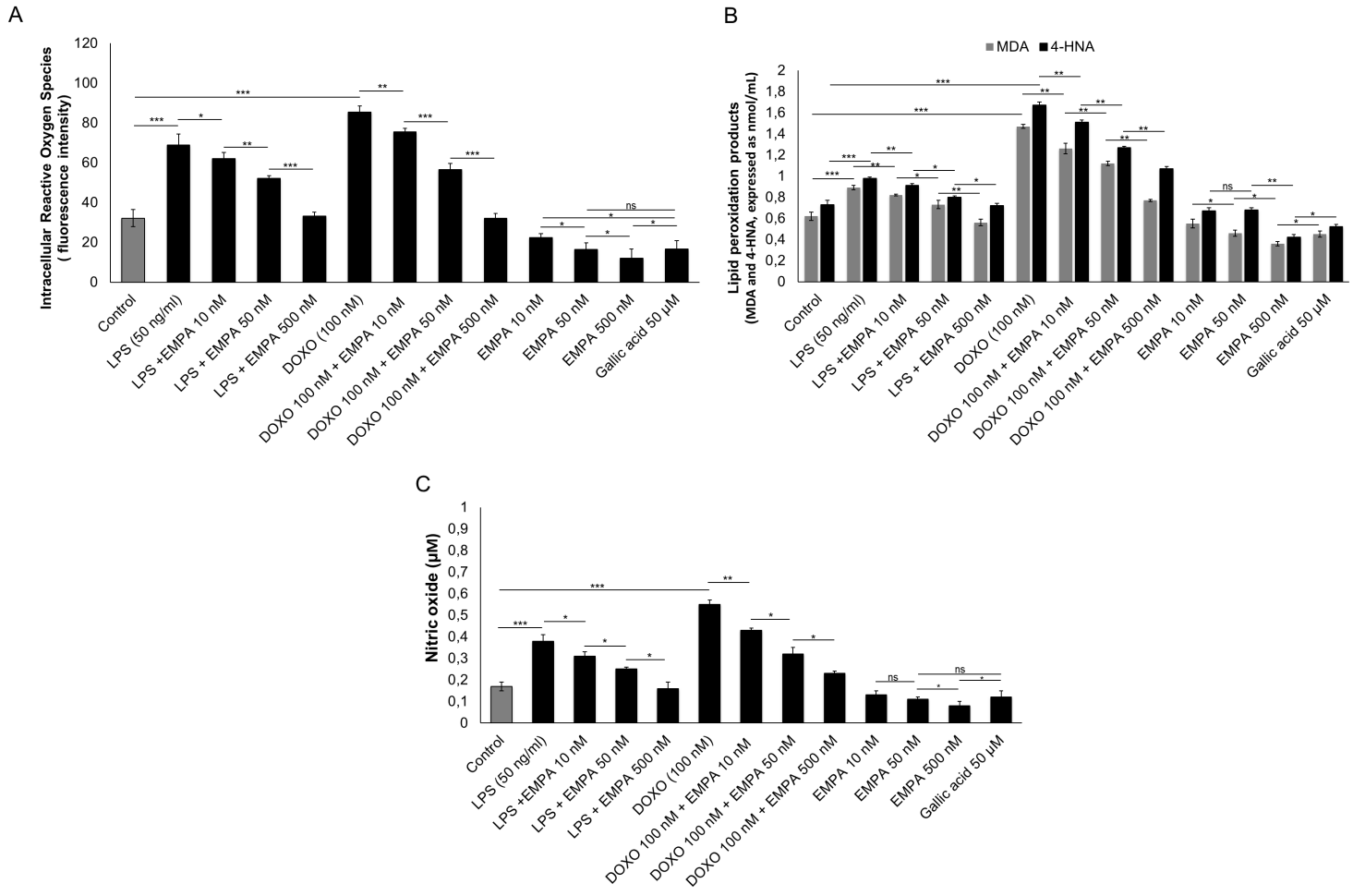

Figure 2

EMPA has anti-oxidant effects on cardiomyocytes under pro-inflammatory conditions (LPS) and under exposure to doxorubicin (DOXO). (A) Intracellular reactive oxygen species (iROS) quantification (expressed as cell fluorescence); (n=3) (B) Quantification of lipid peroxidation products (4-HNA and MDA) (expressed in nmol/mL) (n=3); (C) Production of nitric oxide (µM) (n=3). Experiments were performed in cardiomyocytes (5x103 cells/well seeded in a 24-well plate) untreated (control) or treated with gallic acid (as positive antioxidant control), EMPA (10, 50, 500 nM), LPS (40 ng/ml) or DOXO (100 nM) alone or co-incubated with EMPA at 10, 50 and 500 nM. One-way ANOVA. Values are expressed ± SD. *** P<0.001; **P<0.01; * P<0.05; ns: not significant.

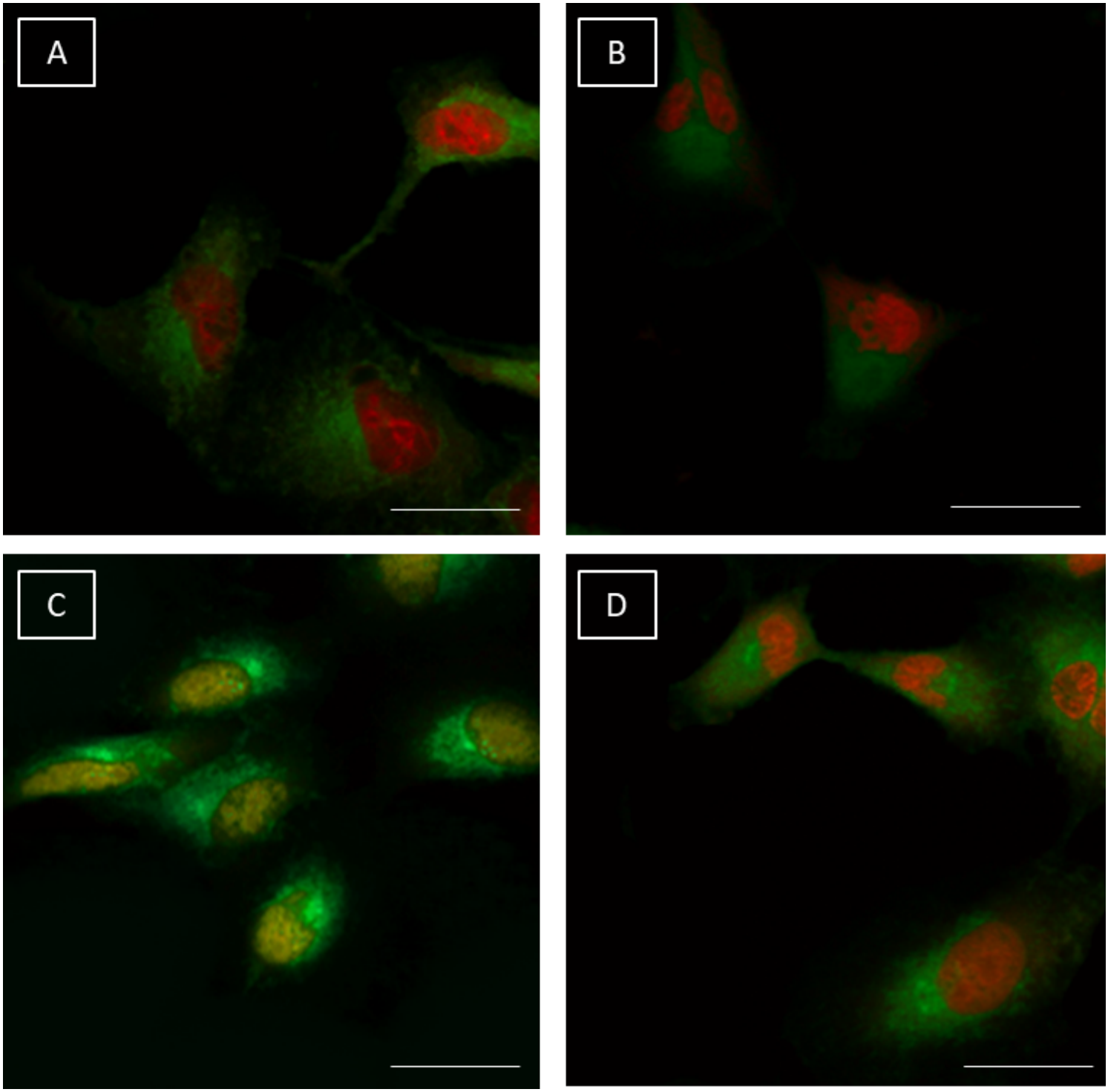

Figure 3

Co-incubation of Empagliflozin (EMPA) and doxorubicin (DOXO) reduced the expression of pro-inflammatory interleukins, leukotrienes and p65/NF-Kb compared to only DOXO-treated cells. For each experiment, 5x103 cells/well were seeded in a 96-well plate; cells were exposed to EMPA (10, 50, 500 nM), LPS (40 ng/ml), DOXO (100 nM) alone or with EMPA at 10, 50 and 500 nM (n=4/group). Expression of (A) Interleukin-8, (B) Interleukin-6 and (C) Interleukin1-β (pg/mL). (D) Leukotriene B4 expression (pg/mL) in cardiomyocytes exposed to arachidonic acid (10 μM), EMPA (10, 50, 500 nM) alone or associated to arachidonic acid, DOXO (100 nM) alone or co-incubated with EMPA at 10, 50 and 500 nM. (E) p65/NF-kB

DNA binding activity, expressed as fold of untreated (control) cells (n=3). (F) MyD88 and NLRP3 expression (fold of control), (n=3) ; One-way ANOVA. Value are expressed ± SD. ***P<0.001; **P<0.01; *P<0.05; ns: not significant. (G): Confocal laser scanning microscope images of cardiomyocytes exposed to medium alone (A), EMPA 100 nM (B), DOXO 100 nM (C) and EMPA (100 nM) DOXO (100 nM) in combination (D) for 24 hours (n=3/group). Green fluorescence indicates p65/NF-kB staining; red fluorescence indicates cell nucleus. Scale bar: 50 µM.

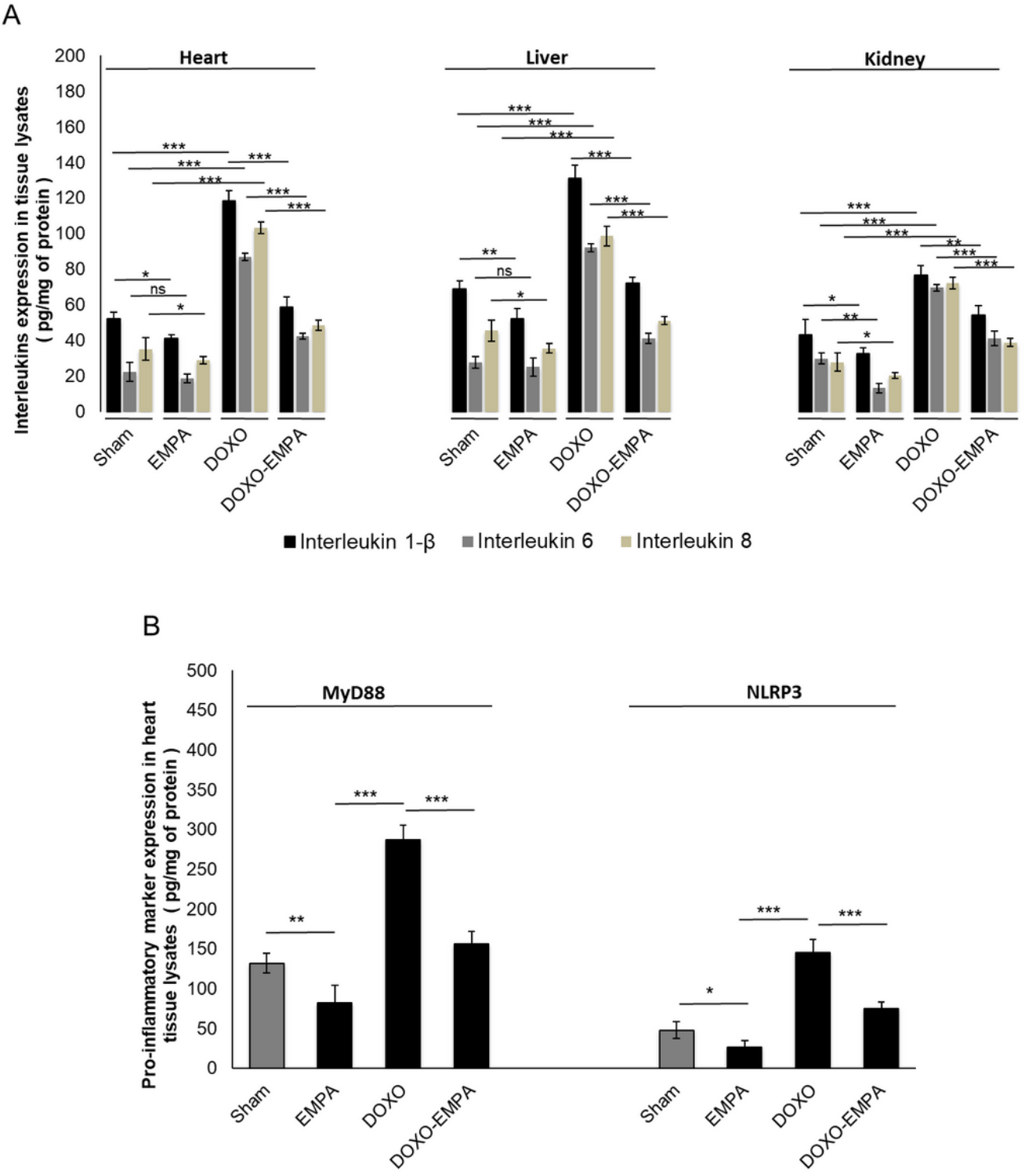

Figure 4

A: EMPA exerts anti-inflammatory effects on the liver, heart and kidney of mice treated with DOXO. B: Empagliflozin reduces pro-inflammatory markers MyD88 and NLRP3 in cardiac tissue during DOXO treatments. For both, we quantified the expression of interleukin 1-β, interleukin 6 and interleukin 8 (pg/mg of protein) in heart, liver and left kidney lysates of mice untreated (Sham) or treated with EMPA, DOXO or DOXO/EMPA for 7 days (n=6 for each group) ; in heart tissues only, we quantified the expression of MyD88 and NLRP3 through mouse ELISA kits (pg of marker/mg of protein). One-way ANOVA. Values are expressed ± SD.*** P<0.001; **P<0.01; *P<0.05; ns: not significant.

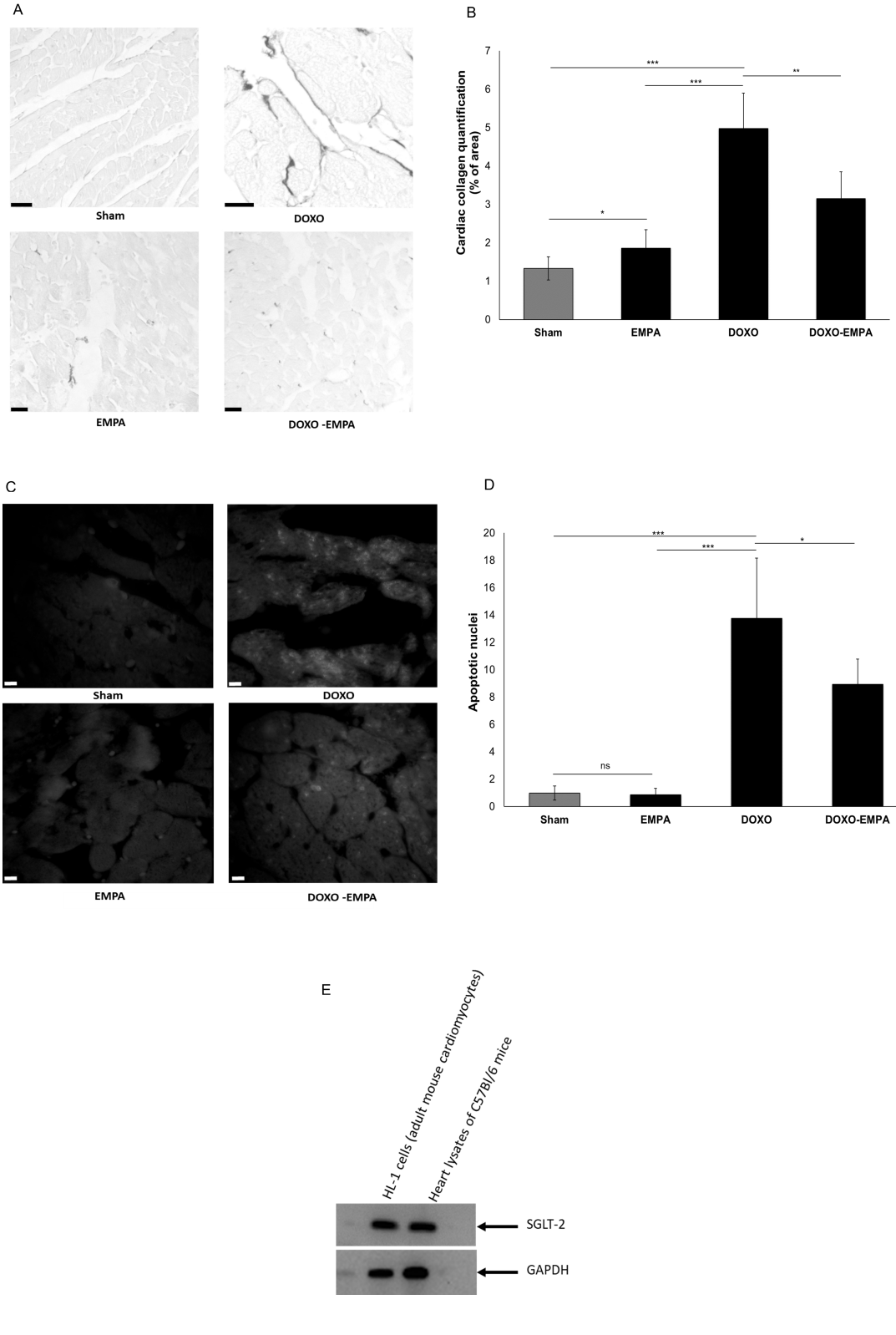

Figure 5

Cardiac histological and cardiac function studies in mice treated with saline solution (Sham), EMPA 10 mg/kg/day, DOXO 2.17 mg/kg/day or EMPA associated to DOXO (n=6 for each group). (A, B) representative images and quantification of the interstitial fibrosis (showing the analysis of collagen, indicative of the fibrosis state) in cardiac tissue ; (C,D) apoptotic nuclei, expressed as relative percentage of positive nuclei, in heart tissue (two-way ANOVA with a Bonferroni post hoc test). (E) SGLT-2 protein expression in HL-1 adult murine cardiomyocytes and cardiac extract of C57B/6 mice through western blot analysis. Values are expressed ± SD. *** P<0.001; **P<0.01; * P<0.05; ns: not significant.

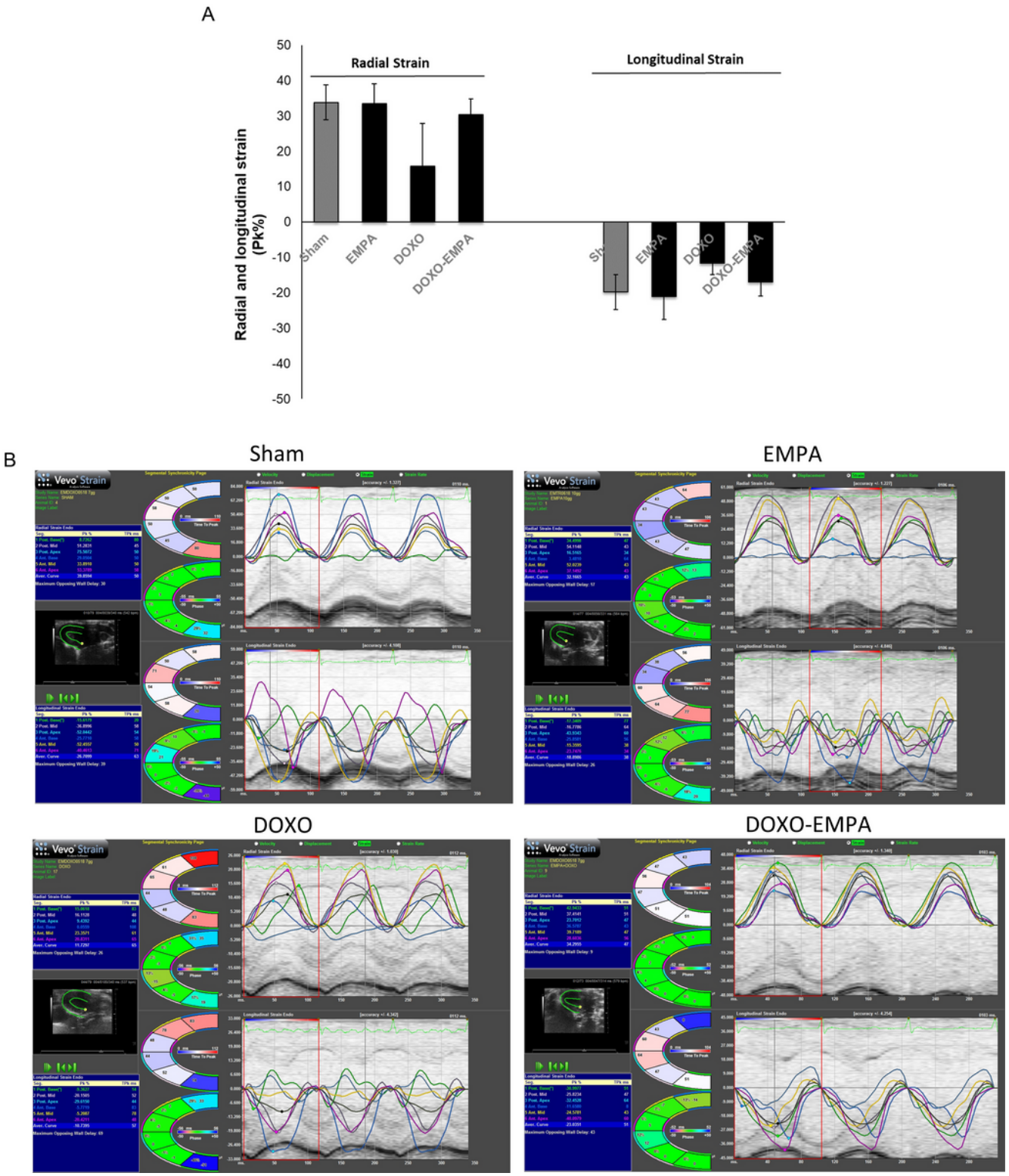

Figure 6

Cardiac function studies in mice treated with saline solution (Sham), EMPA 10 mg/kg/day, DOXO 2.17 mg/kg/day or EMPA plus DOXO (n=6 for each group). (A) Radial and Longitudinal Strain are expressed as Pk (%). (B): representative radial and longitudinal strain images for each group. (two-way ANOVA with a Bonferroni post hoc test) . Values are expressed ± SD. *** P<0.001; **P<0.01; * P<0.05; ns: not significant.

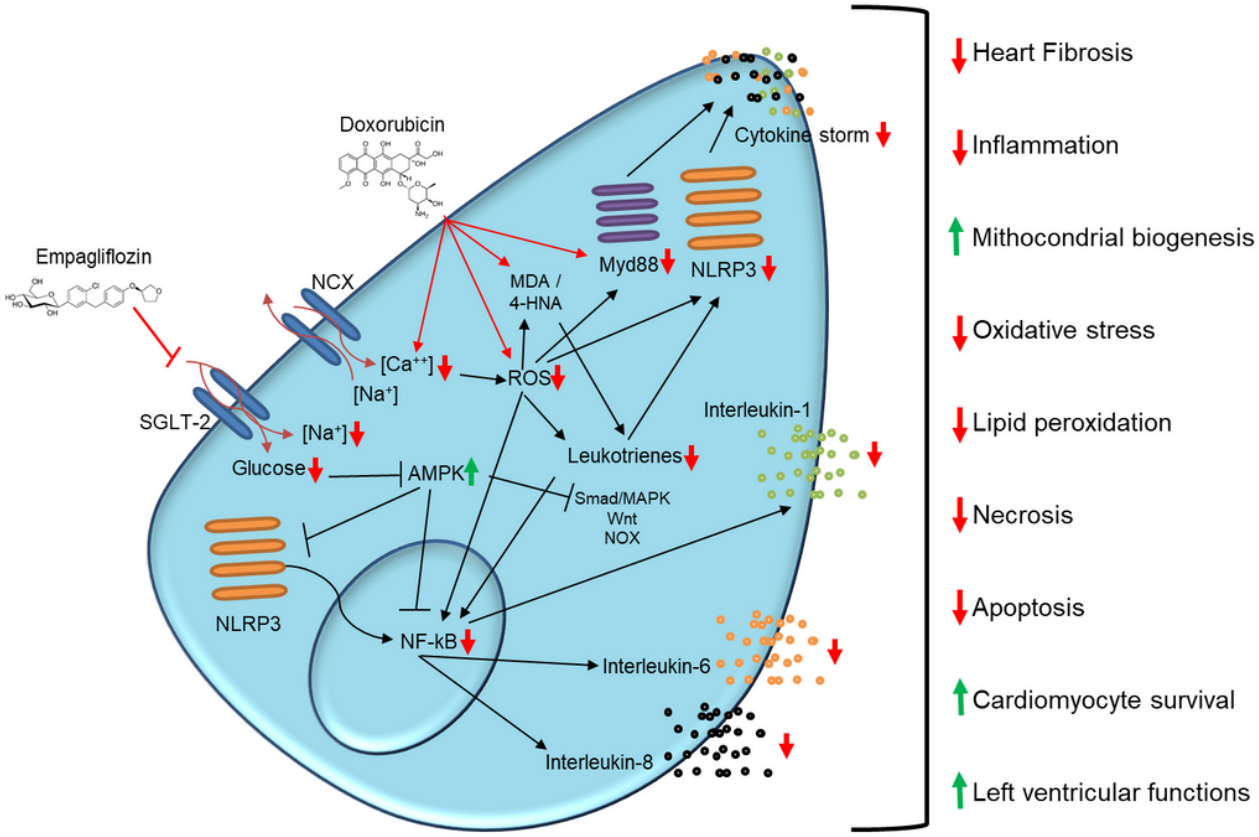

Figure 7

Mechanisms of action of empagliflozin against doxorubicin-induced cardiotoxicity. Empagliflozin inhibits the activity of SGLT-2 thereby reducing intracellular glucose and sodium in cardiomyocytes, resulting in the inhibition of iROS, lipid peroxidation and NLRP3/MyD88-related pathways; the inhibition of NLRP3 and NF-kB reduces the pro-inflammatory cytokine storm in cardiomyocytes exposed to DOXO.